

# AstroSat Observation of Recent Outburst in the Be/X-ray Binary LS V +44 17/RX J0440.9+4431

Arshad Hussain,<sup>1,\*</sup> Akash Garg,<sup>2,†</sup> Ranjeev Misra,<sup>2,‡</sup> and Umananda Dev Goswami<sup>1,§</sup>

<sup>1</sup>*Department of Physics, Dibrugarh University, Dibrugarh 786004, Assam, India*

<sup>2</sup>*Inter-University Centre for Astronomy and Astrophysics, Post Box No. 4, Ganeshkhind, Pune-411007, India*

A Be/X-ray binary system known as RX J0440.9+4431 (or LS V +44 17) is a potential member of the uncommon gamma-ray binary class. With an orbital period of 150 days, this system consists of a neutron star and a Be star companion. The MAXI observatory discovered an X-ray outburst from the source in December of 2022. Early in January, the outburst reached its peak, which was then followed by a decrease and a subsequent rebrightening. The X-ray flux exceeded 1 Crab in the 15-50 keV range at this second peak. AstroSat observations were conducted close to the peak of the second outburst, from January 11 to January 12, 2023. We report here the results of our search for 3-80 keV X-ray emission in the data of the AstroSat's LAXPC detector. It is found that the pulse period of the source is around 208 seconds. The source is found to be emitting more in the softer part of the X-ray energy range. The spectral characteristics can be described by employing a power-law model with an exponential cutoff, along with a blackbody component, interstellar absorption and an additional 6.4 keV iron fluorescence line.

Keywords: Be/X-ray binary; AsroSat's LAXPC; Temporal and spectral behaviours

## I. INTRODUCTION

X-ray binaries (XRBs) are the peculiar X-ray systems among the most puzzling and brightest objects in the Universe. XRBs can be simply defined as systems that consist of a compact object (black hole or neutron star) and an optical companion (typically a normal main-sequence star) which are gravitationally bound to each other [1–4]. They are “close” systems due to mass transfer from the companion to the compact object [5]. X-ray binaries can be divided into low-mass and high-mass XRBs depending on the donor star's mass. In the case of low-mass XRBs (LMXBs) ( $M \leq 1 M_{\odot}$ ), the accretion of materials happens through Roche-lobe overflow of the companion star [5, 6]. For high-mass XRBs (HMXBs) ( $M \geq 5 M_{\odot}$ ), the accretion takes place through stellar wind or Be-disk of the donor star [1]. They contain early-type stars as companions, such as O or B stars and are strong X-ray emitters. Based on the luminosity class, the HMXBs can be further subdivided into Be/X-ray binaries (BeXBs), where the optical companion can be a dwarf, giant, or sub-giant OBe star in the luminosity classes III-IV, and supergiant XRBs (SGXBs), in which the companion is a luminosity class I-II supergiant star [1, 5]. Moreover, in BeXBs, the optical partners are fast-rotating stars of the type mentioned above with distinctive emission lines in their spectrum at some point of their existence (accordingly the lowercase “e” used to denote emission) [5, 7–9]. Usually, the neutron star as the compact object in the binary system is considered as a defining characteristic of BeXBs. These non-supergiant BeXBs possess larger orbital periods [1, 5]. Roughly two-thirds of HMXBs populations are Be/X-ray binaries [1]. In the binary systems known as the accreting X-ray pulsars (XRP), a neutron star accretes matter from the donor companion. The vast majority of XRP fall under the subclass of Be/X-ray binaries. Here, the companion's circumstellar disk emits H $\alpha$  Balmer lines at least once in its life [7, 10, 11]. In BeXBs, the optical emissions predominantly come from the Be star, whereas the X-ray emissions provide insights into the conditions in the vicinity of the neutron star [11, 12]. BeXBs systems exhibit two different X-ray outburst types: Type-I and Type-II X-ray outbursts. Type-I commonly occurs during the periastron passage of the neutron star, while Type-II can occur at various orbital phases which may be linked to the warping of the circumstellar disk's outermost region [12].

RX J0440.9+4431 is a BeXB which was discovered by Motch et al. in 1997 [13] during the ROSAT's survey of the galactic plane [1, 14]. Its distance was estimated to be  $\sim 3.3 \pm 0.5$  kpc [1]. Strong X-ray emissions ( $\sim 10^{34-35}$  erg s<sup>-1</sup>) [14] with pulsations (period  $\sim 202.5 \pm 0.5$  s [15]) were discovered from this source which confirmed it as an X-ray pulsar [15, 16]. Reig et al. (2005) [16, 17] had done a thorough investigation of the characteristics of its optical counterpart. This optical companion, BSD 24-491/LS V +44 17, was classified as a Be star which belongs to the B0.2V spectral class [1, 17]. Due to the occurrence of the limited number of relatively dim Type-I outbursts (which is typical for BeXBs) that have been observed, the characteristics of this binary system have not been extensively investigated in the X-ray domain [16, 18–20]. RX J0440.9+4431 stands out as one of the rare X-ray binary systems where accretion continues even during quiescence [15, 16, 21]. It is crucial to note that the accretion in quiescent is powered by a cold and non-ionized disk [16, 22] along with the wind accretion.

The MAXI detector observed the first outburst from RX J0440.9+4431 during March 26, 2010 and April 15, 2010 [11, 14, 18] with a peak luminosity of  $3.9 \times 10^{36}$  erg s<sup>-1</sup> (3-30 keV) [14, 23]. *Swift*/BAT also detected the next two minor X-ray flares

\* arshad007h@gmail.com

† akash.garg@iucaa.in

‡ rmisra@iucaa.in

§ umananda2@gmail.com

following this first outburst [11, 24]. It is remarkable to note that considering the RX J0440.9+4431 is located at a distance of  $2.44_{-0.08}^{+0.06}$  kpc [14, 25], the observed luminosity of the source was found to be remained considerably below the characteristic  $10^{37}$  erg s<sup>-1</sup>, which is typically associated with Type-I outbursts in the case of BeXBs [5, 14, 24, 26–28].

The transient activity exhibited by the source was observed mainly in the years 2010 and 2011 [16] with luminosity peaks varying from  $(1-5) \times 10^{36}$  erg s<sup>-1</sup>. During this span of time, the presence of a probable cyclotron line was reported as an absorption feature at  $\sim 30$  keV which denotes a magnetic field intensity of  $3 \times 10^{12}$  G [14, 19]. However, later studies have raised questions about the presence of this specific spectral feature [16, 20]. The pulse profile that was recorded displayed a generally simple and nearly sinusoidal pattern in 0.3-60 keV range. Nevertheless, some luminosity-dependent structures were evident in the 3-15 keV range [16, 19]. Usui et al. (2012) [23] noted an abrupt fall of luminosity after the initial peak. This was described as a consequence of the accretion stream blocking the emission zone. The source was most likely in a sub-critical accretion condition, meaning that the emission originated from a hotspot, as evidenced by the relatively low measured luminosity and very simple shape of the pulse profile [16, 29]. The soft X-ray spectra were also observed by various observatories. The spectra can be explained as a composite model of power-law and black-body components with the addition of the 6.4 keV iron line [14, 19, 21, 23].

After more than ten years of inactivity, RX J0440.9+4431 went through a massive Type-I outburst on December 29, 2022, which was detected by the MAXI all-sky monitor [30]. This was followed by a multi-wavelength campaign using NuSTAR, NICER, Chandra, *Swift*-XRT, and AstroSat which lasted for almost four months [14, 30–33]. *Swift*/BAT data indicates that on January 4, 2023, the outburst peaked  $\sim 0.6$  Crab in the 15-50 keV band with luminosity  $\sim 5 \times 10^{36}$  erg s<sup>-1</sup>. The source then had a rapid drop in luminosity until the trend changed around January 13, 2023, indicating the start of a significant Type-II outburst. This outburst achieved its peak of  $\sim 2.2$  Crab on January 20, 2023, having a luminosity of  $\sim 2 \times 10^{37}$  erg s<sup>-1</sup> in the 15-50 keV band [14, 32]. The source was observed by AstroSat LAXPC on January 11, 2023 [34]. In this paper, we report the results of the analysis of this observational data of RX J0440.9+4431.

The remaining part of this paper is organized as follows. In Section II, we provide a summary of the instrument, the observation data used and the data reduction procedure. The temporal and spectral analysis of the LAXPC data are presented in the Section III. The Section IV is devoted to discuss the results of both timing and spectral analysis in more detail. In Section V, we summarise our findings.

## II. LAXPC DETECTORS, OBSERVATIONS AND DATA REDUCTION

### A. LAXPC

India's first multi-wavelength astronomical observatory, the AstroSat, has been in active operation for about the last eight years. Launched by the Indian Space Research Organisation (ISRO) on September 28, 2015, it was placed in a circular orbit at an altitude of 650 km above the Earth's surface with a 6° inclination and an orbital period of 98 minutes. AstroSat uses a collection of four equipment, which includes a UV imaging telescope and three X-ray sensors all of which cover a range of energies from around 1 eV to 100 keV [35]. The hard X-ray instrument, the Large Area X-ray Proportional Counter (LAXPC) is one of the three X-ray sensors [36–38]. It consists of three identical large-area proportional counters that are co-aligned, each having multilayer geometry [36, 37, 39] and with a collection area of  $100 \times 36$  cm<sup>2</sup> [40]. The detectors are identified as LX10 (or LAXPC10), LX20 (or LAXPC20) and LX30 (or LAXPC30). Each detector is equipped with five anode layers which are divided into seven anodes, A1-A7, the upper two layers each having two anodes. On each of the three sides of the detector, there are three veto anodes, A8-A10, as well [36]. A gas mixture of 90% xenon and 10% methane kept at a pressure of around 2 atmospheres, fills the entire volume of LAXPC10 and LAXPC20 detectors. In contrast, a gas combination composed of 84.4% xenon, 9.4% methane and 6.2% argon is present in LAXPC30, which is also kept at a pressure around 2 atmospheres [40].

The LAXPC operates within the energy range of 3-80 keV. The lower energy threshold of this set of devices is influenced by the negligible transmission of X-ray (below 3 keV) through 50  $\mu$ m thick aluminized mylar. On the other hand, the reduced detection efficiency at higher energy leads to the higher energy threshold [41]. The LAXPC possesses the capability to study fluctuations in kHz scale at a high counting rate. A large photon collection area with robust detection efficiency over the complete energy range is necessary for this. The effective area of all three units is  $\sim 4500$  cm<sup>2</sup> at  $\sim 5$  keV,  $\sim 6000$  cm<sup>2</sup> at  $\sim 10$  keV and  $\sim 5000$  cm<sup>2</sup> at  $\sim 40$  keV [41, 42].

This instrument's main objectives are broadband spectrum observations and high-time-resolution research to examine rapid changes in intensity. This is accomplished by the instrument's ability to precisely identify each observed X-ray photon's arrival time, with an accuracy of 10  $\mu$ s. Additionally, it uses a 1024-channel pulse-height analyser to calculate each photon's energy [42]. Agrawal (2006) [37] and Singh et al. (2014) [38] both provide detailed descriptions of the AstroSat observatory and its equipment. Yadav et al. (2016) [39], Agrawal et al. (2017) [41], and Roy et al. (2016) [43] give a more thorough explanation of the characteristics of the LAXPC instrument. Antia et al. (2017) [40] provides comprehensive information on calibration specifications.

## B. AstroSat Observation

AstroSat monitored the source RX J0440.9+4431 from 11:52:07.64 UT on January 11, 2023 to 00:43:20.53 UT on January 12, 2023, covering its eight orbits. In terms of Modified Julian Day (MJD) this observation of AstroSat lies within the MJD period 59955.49 to 59956.03. Background data used for this source was collected between May 2, 11:55:52.52 UT to May 3, 09:50:52.35 UT in the year 2022. This background data was obtained by pointing the instrument at a region devoid of any sources. The background data have been used for obtaining the source's background-subtracted light curve. We obtain all these data from the archival of the AstroSat in the Indian Space Science Data Centre (ISSDC) [34]. It should be mentioned that between 2022 and 2023, MAXI/GSC detected a strong X-ray burst from RX J0440.9+4431 in the 2 to 20 keV energy range [18]. Fig. 1 shows the source's one-day binned MAXI/GSC light curve in 2-20 keV from MJD 59500.0 to MJD 60200.0 [18, 44]. It is coupled with the AstroSat observation on MJD 59955.49 as mentioned above, denoted by a thick red vertical line. The source was about to have a Type-II outburst when the AstroSat observation was made, as seen from the MAXI/GSC light curve.

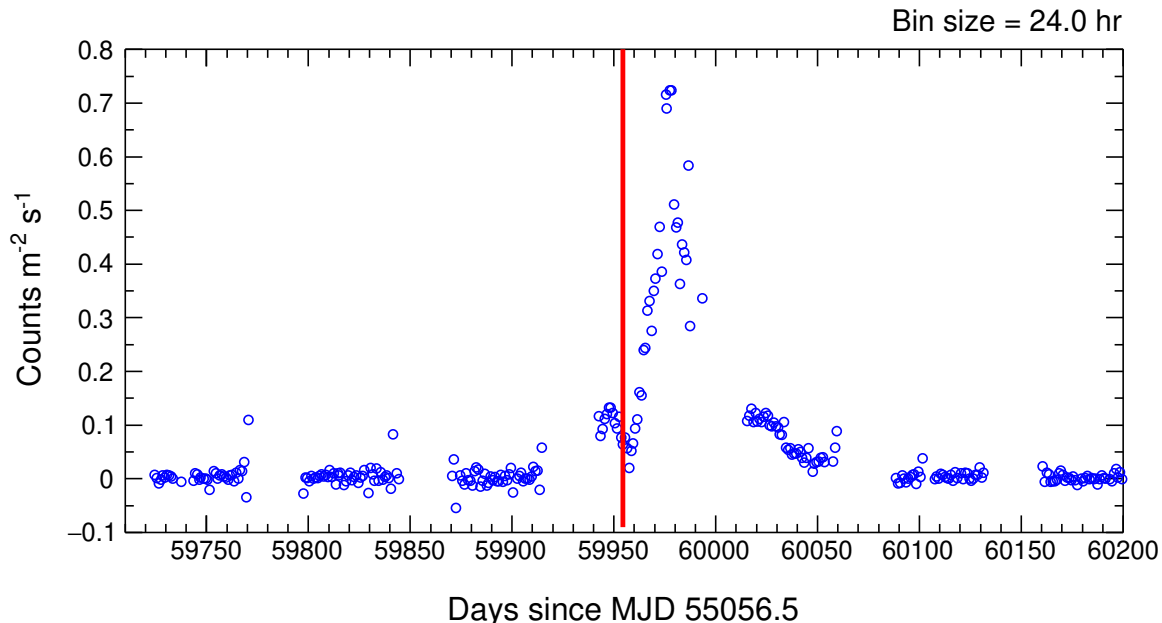


FIG. 1. The light curve of the RX J0440.9+4431 observed by MAXI/GSC during the period of 2022 to 2023 [18, 44]. A significant and substantial outburst event was identified emanating from RX J0440.9+4431 within the energy range of 2 to 20 keV. The vertical strip indicates the specific time period of the AstroSat observations.

## C. Data Reduction

The data reduction process was carried out using the LAXPC data reduction pipeline software “LAXPCsoftware22Aug15”. The “laxplevel2datapipeline” utility was used to convert Level-1 raw data files into Level-2 data. Data was analysed for each of the three LAXPC units individually. The Level-2 data consists of light curve, information about each detected X-ray photon, pulse height and the originating anode layer in (i) broadband counting mode (modeBB), (ii) event mode (modeEA), and (iii) mkf files (which stores housekeeping data and parameter files). Using the LaxpcSoft standard tasks, the light curves and energy spectrum were obtained from the Level-2 event file. The software routine generates the Good Time Interval, which contains timing details for Earth occultation and the South Atlantic Anomaly. We utilise average background counts to determine the source light curve with the background subtraction process. In addition to background correction, to account for the variations in the arrival times of the photons due to the motion of the Solar system, these photon arrival times have undergone barycentric correction to the Solar system barycenter using the AstroSat barycentric correction utility “as1bary”. It requires HEASOFT software [45] package version 6.17 or higher. We use the latest version (6.30.1) available at the time of our analysis. HEASOFT incorporates various tools and programs. XRONOS tool [46] was used for the timing analysis. FTOOLS [47] were primarily used for general data extraction and analysis. The XSPEC package [48] played a key role in spectral analysis. We use data only from the LAXPC20 detector as LAXPC30 was impacted by gas leakage and hence turned off on March 8, 2018 due to

anomalous gain fluctuations. We did not include the data from LAXPC10 as it was operating at low gain [49, 50]. We pick the 3-30 keV energy band for the spectrum since the background is dominant above the 30 keV.

### III. ANALYSIS OF DATA

#### A. Timing Analysis

The light curve of the source was produced from the above-mentioned AstroSat data, i.e. the data obtained from all the observations of LAXPC20 by using the 10 seconds averaged count rates in the 3-80 keV band, which is presented in the top panel of Fig. 2. To have the best signal-to-noise ratio, we extract data only from the top layer of the LAXPC20 instrument. As mentioned earlier, there are eight orbits of observation and for those combined orbits, we also generate the corresponding backgrounds shown in the middle panel of Fig. 2. The background varies between  $\sim 48 - 61$  counts  $s^{-1}$  during the observations. To get the final light curve, this background was subtracted from the light curve using the “lcmath” tool. The background-subtracted light curve is shown in the bottom panel of Fig. 2. For clarity in the visibility of pulsations the first segment of the light curve of Fig. 2 is also shown in Fig. 3. Pulsations of X-rays from the source are distinctly visible in the light curve from both figures.

Employing the FTOOL subroutine “powspec” in HEASOFT, the one-second binned power density spectrum (PDS) of the source was generated using the light curve of the source given by the LAXPC20 detector. We divide the light curve into stretches of 1024 bins per interval. The final PDS was created by averaging the PDSs from all the segments. The generated PDS has a very significant peak at  $\sim 0.005$  Hz corresponding to the source’s spin period of  $\sim 200$  s (see Fig. 4). The PDS shows no quasi-periodic oscillation (QPO) [5] peaks since no additional nearby significant peaks have been observed except few harmonics in the spectrum. Applying the standard  $\chi^2$  maximization approach with the FTOOLS job “efsearch” a more accurate estimation of the pulse period can be obtained. The period was searched around 200 s as approximated in the PDS generated from the light curve. It was found to be 207.93 s (see Fig. 5) confirming the pulse period detected by the NICER mission [1].

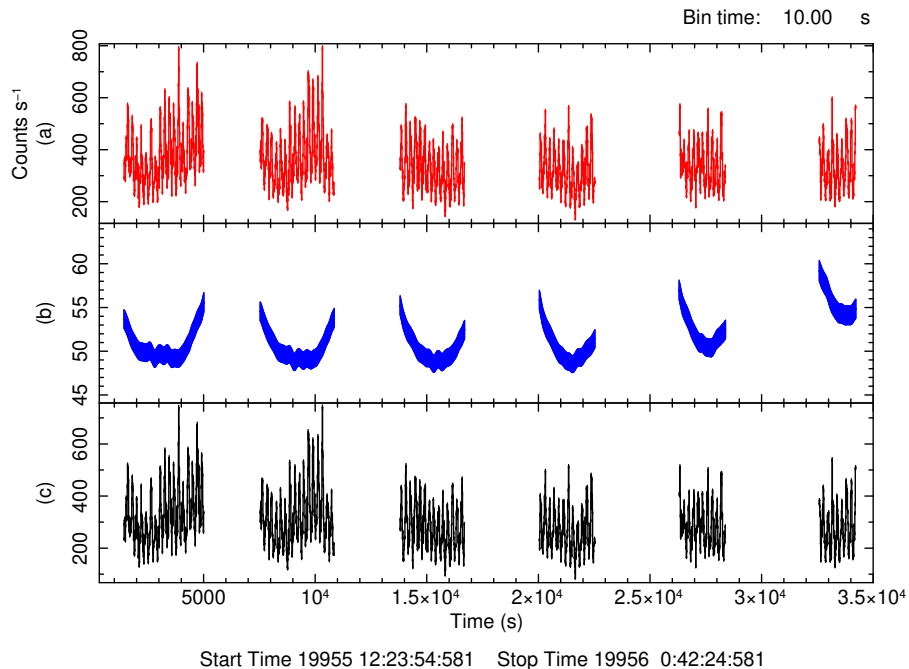


FIG. 2. (a) Light curve of the X-ray source RX J0440.9+4431 including the background count rates. (b) Background light curve. (c) Background subtracted light curve of the source. The gaps in the light curve is due to the passage of the satellite through the South Atlantic Anomaly regions. In these plots, 10 s binning is used in the energy range of 3-80 keV.

To investigate how intensity fluctuations depend on energy, light curves were produced within five unique energy bands: 3-12 keV, 12-20 keV, 20-30 keV, 30-50 keV and 50-80 keV for the LAXPC20 detector. Only Layer 1 data were utilised for the construction of the light curves in the energy range from 3 to 20 keV. This selection was considered due to the fact that most incident photons ( $\sim 90\%$ ) with energy  $< 20$  keV are likely to be absorbed in Layer 1 [42]. Similar to this, light curves in the 20 to 50 keV range were produced by summing data from Layers 1 and 2, while those in the 50 to 80 keV range used data from

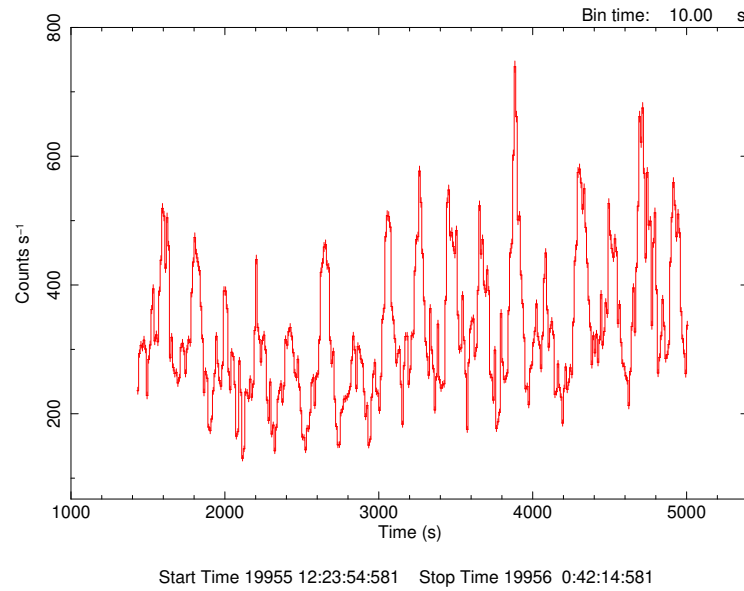


FIG. 3. Time scale amplified background-subtracted light curve of the source RX J0440.9+4431 in 3-80 keV energy range obtained by using the 10 s bins.

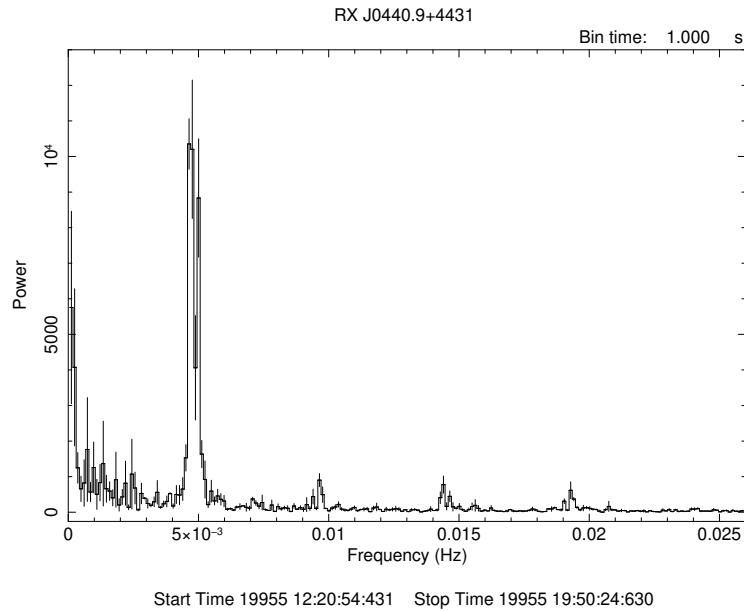


FIG. 4. The power density spectrum of RX J0440.9+4431 generated by using the LAXPC20 data from 10 s binned barycenter corrected light curve in 3-80 keV energy band. A strong pulsation with a peak at  $\sim 0.005$  Hz was found in the PDS.

all five layers. The count rates for the LAXPC20 detector within these five energy bands are shown in Table I. Fig. 6 shows that the higher amplitudes of oscillations are noticeable in the energy bands of 3-12 keV, 12-20 keV and 20-30 keV than in the 30-50 keV and 50-80 keV bands.

To analyse the spectral evolution during the intensity oscillations, hardness ratios (HRs) were computed. These HRs are defined as the count rates in a higher energy band divided by the count rates in a lower energy band. We generate four hardness ratio diagrams (background subtracted) for 12-20 keV/3-12 keV, 20-30 keV/12-20 keV, 30-50 keV/20-30 keV and 50-80 keV/30-50 keV. In Fig. 7, it is noteworthy to notice that the source's intensity shows no correlation with the HR. It indicates that the intensity oscillations are not directly related to spectral changes within the detected energy ranges.

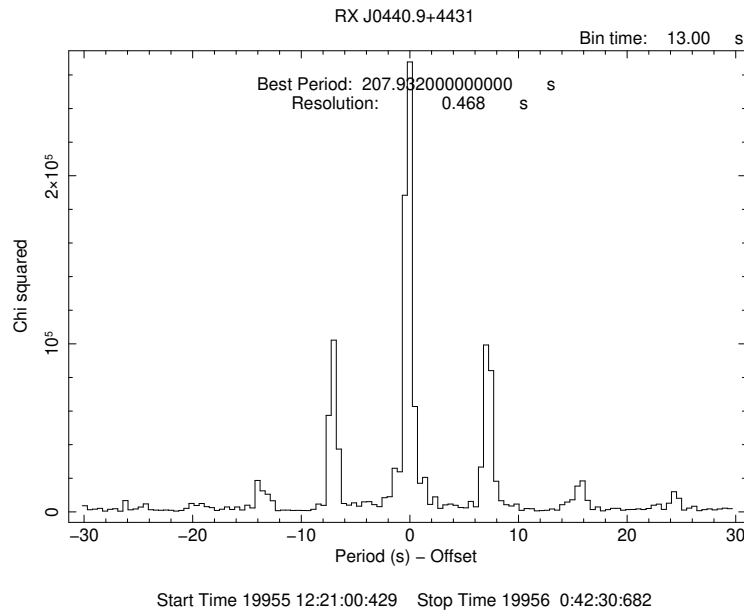


FIG. 5. The pulse period of the pulsar RX J0440.9+4431 estimated by using the FTOOLS subroutine “efsearch” from the LAXPC20 data’s light curve. The period was found to be around 207.932 s.

TABLE I. Background subtracted LAXPC20 count rates in five energy bands of the source RX J0440.9+4431.

Energy Range (keV)	Average Count Rate (counts s <sup>-1</sup> )
3-12	240.41
12-20	53.57
20-30	17.75
30-50	18.88
50-80	16.73

## B. Spectral Analysis

Since the spectral response matrix of the LAXPC20 detector is well determined, we only conduct a thorough spectral analysis on LAXPC20 data. The spectral fitting and statistical analysis are done using the XSPEC version 12.12.1. Data from all the eight orbits observed by LAXPC20 were merged to derive the spectrum of the source in the energy band ranging from 3 keV to 80 keV. To maximize the inclusion of X-ray photons and to minimize the background, the spectrum was generated only from the top layer of LAXPC20. The background spectrum was found to be dominating above 30 keV. Therefore, the photons below 3 keV (ignored channel: 1) and above 30 keV (ignored channels: 30-77) for LAXPC are ignored to avoid larger systematic errors. The LAXPC software has a single routine to generate the source spectra, the background spectra and the response matrix files. The spectra were fitted with a combination of models “TBabs\*(cutoffpl + bbodyrad + gaussian)” which are built-in models found in XSPEC.

To model the spectrum, we first consider a single-component model, the power-law model with an exponential cutoff (cutoffpl). Even after using a systematic error of 0.02 (i.e. 2%) in data, it gives a poor fit with  $\chi^2/\text{dof}$  value of 5056/25. Next, we add a blackbody radiation model (bbodyrad) to the power-law model. With this addition, we gain a noticeable improvement in fitting parameters ( $\chi^2/\text{dof} = 2723.11/23$ ). However, the combined model left a residual at  $\sim 6.4$  keV. Therefore a Gaussian line at 6.4 keV (due to iron  $K\alpha$  line) was included which significantly improved the fit with  $\chi^2/\text{dof} = 270.98/20$ . Finally, we include the multiplicative model, TBabs [51, 52] for interstellar absorption. Here the column density value has been fixed at  $N_H = 1.0 \times 10^{22} \text{ cm}^{-2}$ . It gives a very good fit of  $\chi^2/\text{dof} = 22.29/20$  (i.e.  $\chi^2_{\text{red}} = 1.11$ ). Table II lists the spectral parameters obtained from the best fit of our combined model. The best-fitted spectrum of the source is shown in Fig. 8.



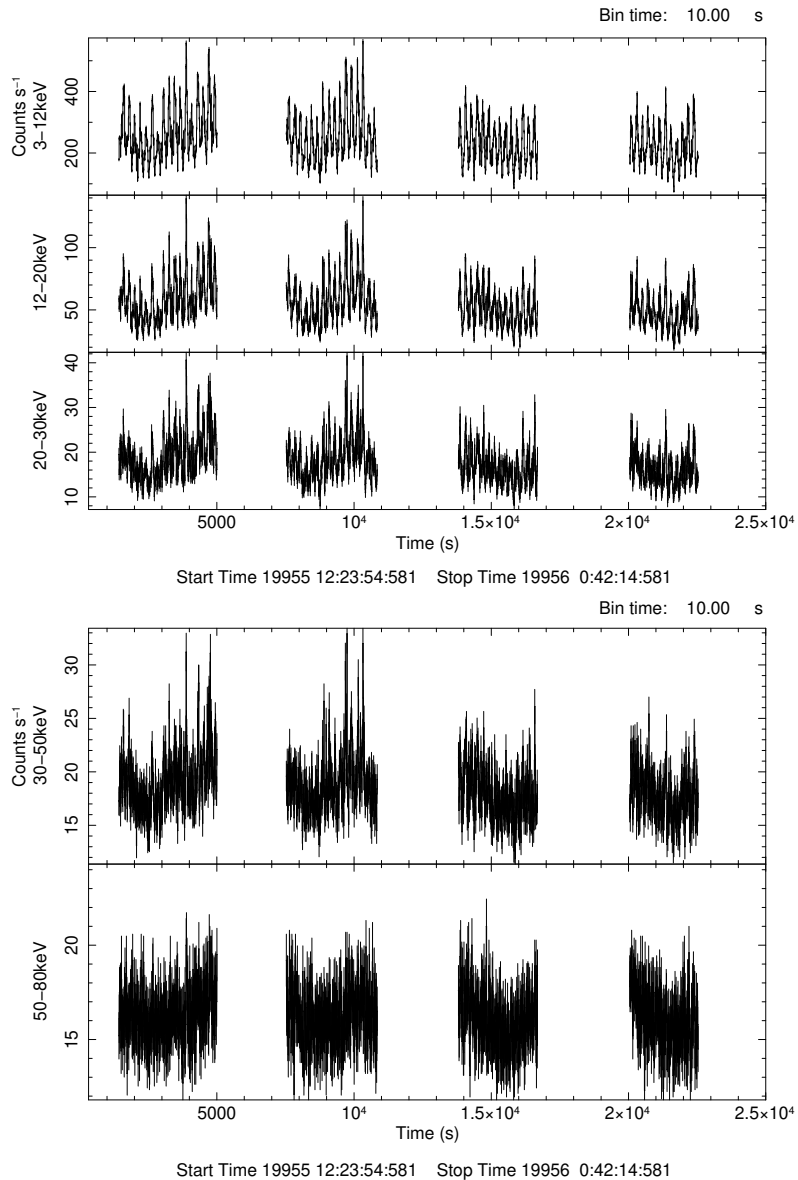


FIG. 6. Background subtracted light curves for (a) 3–12 keV, (b) 12–20 keV, (c) 20–30 keV, (d) 30–50 keV and (e) 50–80 keV for LAXPC20 data of the pulsar RX J0440.9+4431.

#### IV. RESULTS AND DISCUSSION

The *AstroSat* observation of RX J0440.9+4431 provides us with an opportunity to investigate the behaviour of the pulsar at X-ray energies 3–80 keV during the enormous outburst in 2023. *Swift*/BAT observations show that the huge outburst reached a record-high flux of 2.3 Crab [1]. During the outburst of the source, cleaned event data were used to create a 10-second binned light curves in various energy ranges to observe the periodicity in the data. According to Reig & Roche in 1999 [15], the source RX J0440.9+4431 has been classified as a persistent BeXB due to its longer spin period and less X-ray variability than typical transient pulsars. In such cases, the neutron star and the Be star are in a wide orbit. The neutron star orbits through the outer portion of the Be circumstellar disc, where matter density is low. However, RX J0440.9+4431 displayed an eruption which was contrary to what was anticipated. This suggests that the source was in transition to a supercritical regime [16, 23].

The light curves of the source clearly exhibit the prominent intensity oscillations of a period of approximately 200 seconds. These oscillations are readily visible across all of the light curve data. The  $\sim 200$  s X-ray pulsations are clearly visible also in the energy-resolved light curves in 3–12 keV, 12–20 keV, 20–30 keV, 30–50 keV and 50–80 keV bands. To search for the periodic signals, the barycentre corrected event data were employed and `efsearch` task in `FTOOLS` was executed. This task folded the light curve over a trial period and identified the most likely period. From this analysis, we obtain a measurement of the pulse

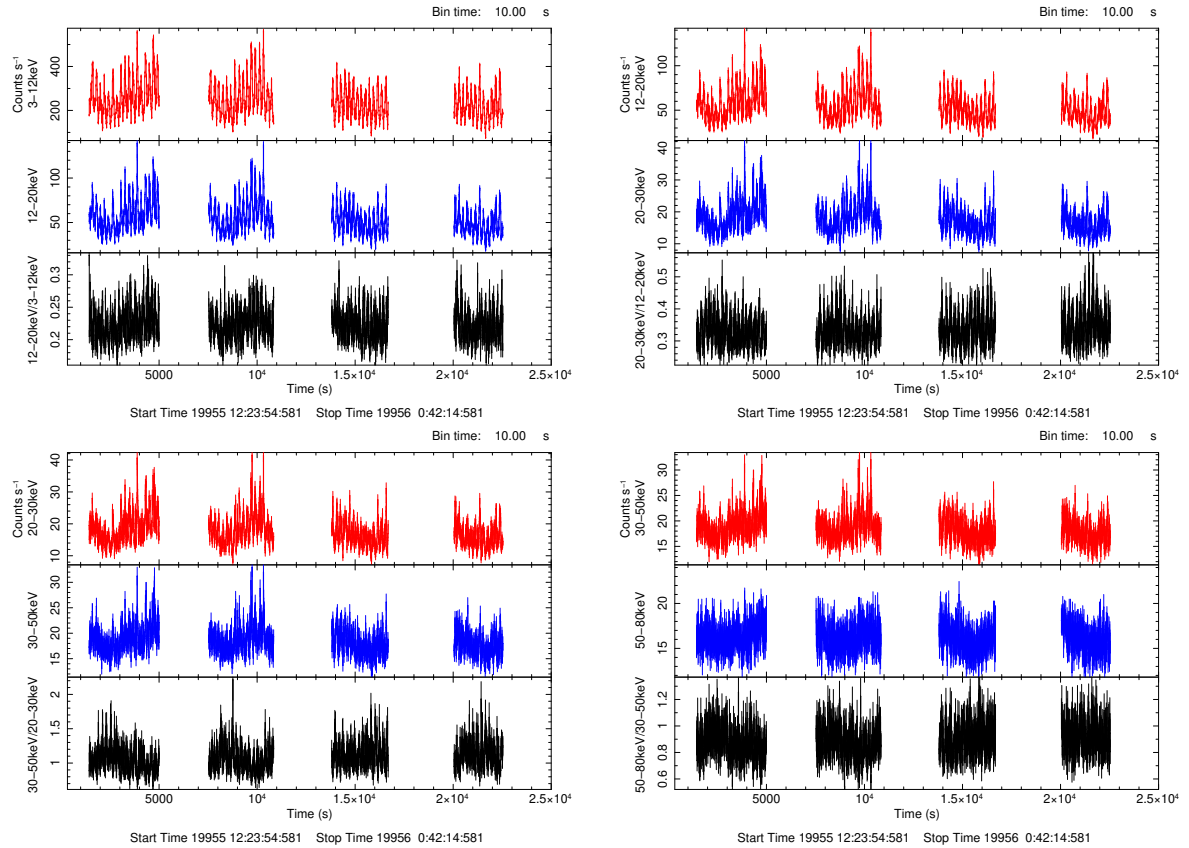


FIG. 7. Hardness ratios for 12-20 keV/7-12 keV (top left panel), 20-30 keV/12-20 keV (top right panel), 30-50 keV/20-30 keV (bottom left panel) and 50-80 keV/30-50 keV (bottom right panel). The bottom section of each panel (black color) represents the hardness ratio of the corresponding energy band.

TABLE II. Best fitting spectral parameters obtained from the model: TBabs\*(cutoffpl + bbodyrad + Gaussian).

Model	Parameter	Value
TBabs	$N_H$ ( $10^{22}$ cm $^{-2}$ )	1.0000
cutoffpl	PhoIndex	0.9495
	HighECut (keV)	19.5063
	Norm	0.1032
bbodyrad	kT (keV)	0.2818
	Norm ( $\times 10^5$ )	1.9452
Gaussian	LineE ( $\times 10^{-15}$ keV)	9.2099
	Sigma (KeV)	4.4204
	Norm	0.1855

period  $\approx 207.9$  s which confirms the pulse period as described by NICER observation for this source [1]. The evolution of the pulse period could not be studied due to AstroSat's observation for a very short period of time. However, Reig & Roche in 1999 [15] found its period to be  $\sim 202.5$  s. According to LaPalombara (2012) [21], the pulse period was  $\sim 204.96$  s. Another study showed its period to be  $\sim 205$  s [23]. Thus, our measured period of 207.9 s in the recent AstroSat observation is notably longer than the one recorded in 1999. This discrepancy suggests that over the previous ten years, the neutron star has been slowing down. This deceleration indicates that the neutron star's rotation rate will gradually slow down over time.

In energy-resolved light curves, the spectral changes can be seen clearly. It is noticed that the source is softer, i.e., it emits more low energy photons, primarily in the 3-12 keV band ( $\sim 240$  counts  $s^{-1}$  on average). This may refer to cold disk accretion in our Be/X-ray binary. Be/X-ray binaries are thought to be persistent systems. This hypothesis supports that the long-term, low-level X-ray activity of these sources is probably due to the accretion of matter onto the neutron star from the winds of the



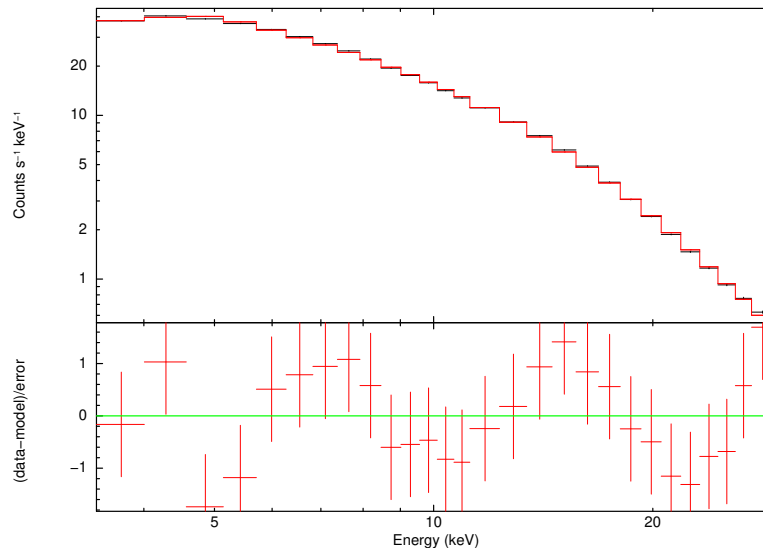


FIG. 8. Fitted LAXPC spectrum of the source RX J0440.9+4431. The best fit is obtained by using the model TBabs\*(cutoffpl + bbodyrad + Gaussian). The fitted model spectrum is shown by the red solid line along with the observed one in black colour. The residuals between the data and the corresponding model predictions are shown in the lower section of the plot.

star. BeXBs sometimes show a periodic increase in X-ray activity rather than being persistent X-ray generators. This is thought to be caused by changes in the size of the equatorial disc of the Be star [5]. During the outburst of such systems, the compact object, i.e., the neutron star and the companion star’s equatorial disk comes into proximity (periastron passage). Thus we get quiescent emission from the source [53].

During the modelling of the RX J0440.9+4431 spectrum, it does not show any presence of narrow absorption features which can be identified as a cyclotron line as reported in earlier studies [14, 19]. At this luminosity of  $2 \times 10^{37} \text{ erg s}^{-1}$  (as observed by *Swift*/BAT) during Type-II outburst in 2023, opting for a power-law model with an exponential cutoff was found to be a feasible choice [14, 54]. It is a characteristic of high accretion rates [14, 55, 56]. The Fe  $K\alpha$  line found at 6.4 keV may be generated through the interaction of the hard X-ray radiation with relatively cooler matter. This line may be associated with iron atoms in a nearly neutral state (composite of Fe II and Fe XVIII) [1, 57–59].

## V. CONCLUSION

Here, using the AstroSat LAXPC data, we present the findings of the brief investigation of the temporal and spectral properties of the BeXB system RX J0440.9+4431 during a giant outburst observed at the beginning of 2023. A shift from the subcritical to supercritical accretion regime can be inferred from the change in the intensity and flux hardness during the outburst. The pulse period of the source was also estimated and it was found to be prominent at 207.9 seconds. A longer pulse time has been observed as compared to the previous measurements, which suggests that the rotation of the neutron star has slowed down during the past ten years. A study of broadband spectra near the outburst was also carried out. The spectra of the source can be modelled using interstellar absorption along with high energy cutoff power-law and blackbody radiation which shows the presence of no narrow absorption features, such as cyclotron lines. The iron line at 6.4 keV shows the presence of nearly neutral iron atoms in the interaction of hard X-ray with colder matter.

Overall, our investigation of the outburst of RX J0440.9+4431 reveals important information on the complicated dynamics of the Be/X-ray binary during severe events and delivers insightful knowledge about its behaviour and spectral properties.

## VI. ACKNOWLEDGEMENT

We express our gratitude to the LAXPC team for their contribution to the development of the LAXPC instrument. In this study, we used the data obtained through the HEASARC Online Service, which was made available by NASA/GSFC, in support of NASA High Energy Astrophysics Programs. This paper also makes use of data from the AstroSat mission of the Indian Space Research Organisation (ISRO), which is archived at the Indian Space Science Data Centre (ISSDC). UDG is thankful to the Inter-University Centre for Astronomy and Astrophysics (IUCAA), Pune, India for awarding the Visiting Associateship of the

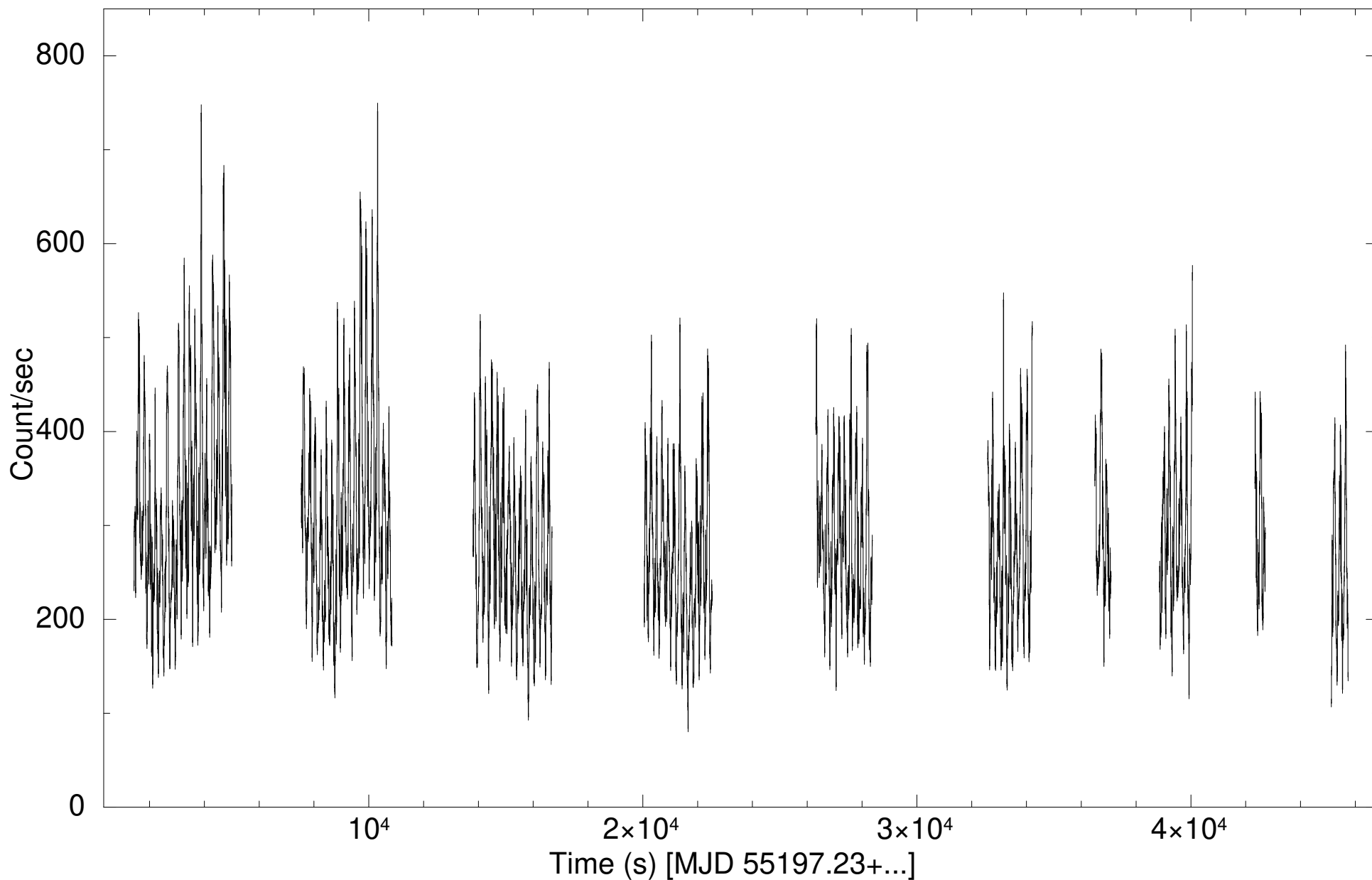
institute.

- 
- [1] M. Mandal et al., *Probing spectral and timing properties of the X-ray pulsar RX J0440.9+4431 in the giant outburst of 2022-2023*, *MNRAS* **526**, 771 (2023).
- [2] F. Nagase, *Accretion-powered X-ray pulsars*, *PASJ* **41**, 1 (1989).
- [3] Q. Z. Liu, J. van Paradijs, E. P. J. van den Heuvel, *A catalogue of low-mass X-ray binaries in the Galaxy, LMC, and SMC (Fourth edition)*, *A & A* **469**, 807 (2007).
- [4] B. Paul, S. Naik, *Transient high mass X-ray binaries*, [arXiv:1110.4446](https://arxiv.org/abs/1110.4446).
- [5] P. Reig, *Be/X-ray binaries*, *Astrophys Space Sci* **332**, 1 (2011).
- [6] N.I. Shakura, R.A. Sunyaev, *Black holes in binary systems. Observational appearance*, *A & A* **24**, 337 (1973).
- [7] J.M. Porter, T. Rivinius, *Classical Be stars*, *PASP* **115**, 1153 (2003).
- [8] L.A. Balona, *The Be phenomenon in early-type stars*, *IAU Colloq.* **175**, 1 (2000).
- [9] A. Slettebak, *The Be stars*, *PASP* **100**, 770 (1988).
- [10] C. Malacaria et al., *Accreting on the edge: A luminosity-dependent cyclotron line in the Be/X-ray binary 2S 1553-542 accompanied by accretion regimes transition*, *ApJ* **927**, 194 (2022).
- [11] J Yan et al., *Long-term optical studies of the Be/X-ray binary RX J0440.9 + 4431/LS V+ 44 17*, *AJ* **151**, 104 (2016).
- [12] A.T. Okazaki, K. Hayasaki, Y. Moritani, *Origin of two types of X-ray outbursts in Be/X-ray binaries. I. Accretion scenarios*, *PASJ* **65**, 41 (2013).
- [13] C. Motch et al., *New massive X-ray binary candidates from the ROSAT Galactic Plane Survey I - Results from a cross-correlation with OB star catalogues*, *A & A* **323**, 853 (1997).
- [14] A. Salganik et al., *RX J0440.9+4431: another supercritical X-ray pulsar*, [arXiv:2304.14881](https://arxiv.org/abs/2304.14881)
- [15] P. Reig, P. Roche, *Discovery of two new persistent Be/X-ray pulsar systems*, *MNRAS* **306**, 100 (1999).
- [16] V. Doroshenko et al., *Complex variations of X-ray polarization in the X-ray pulsar LS V +44 17/RX J0440.9+4431*, [arXiv:2306.02116v1](https://arxiv.org/abs/2306.02116v1)
- [17] P. Reig et al., *Long-term optical/IR variability of the Be/X-ray binary LS V +44 17/RX J0440.9+4431*, *A & A* **440**, 1079 (2005).
- [18] M. Morii et al., *Rebrightening of 1 Crab from LS V+44 17 observed by Swift/BAT and NICER*, *The Astronomer's Telegram* **2527**, 1 (2010).
- [19] S.S. Tsygankov, R.A. Krivonos, A.A. Lutovinov, *Broad-band observations of the Be/X-ray binary pulsar RX J0440.9+4431: discovery of a cyclotron absorption line*, *MNRAS* **421**, 2407 (2012).
- [20] C. Ferrigno et al., *RX J0440.9+4431: a persistent Be/X-ray binary in outburst*, *A & A* **553**, A103 (2013).
- [21] N. La Palombara et al., *XMM-Newton observation of the persistent Be/NS X-ray binary pulsar RX J0440.9+4431*, *A & A* **539**, A82 (2012).
- [22] S.S. Tsygankov et al., *Stable accretion from a cold disc in highly magnetized neutron stars*, *A & A* **608**, A17 (2017).
- [23] R. Usui et al., *Outburst of LS V +44 17 observed by MAXI and RXTE, and discovery of a dip structure in the pulse profile*, *PASJ* **64**, 79 (2012).
- [24] R. Krivonos et al., *The continued flaring activity of LS V +44 17/RX J0440.9+4431*, *The Astronomer's Telegram* **2828**, 1 (2010).
- [25] C.A.L. Bailer-Jones et al., *Estimating distances from parallaxes. V. Geometric and photogeometric distances to 1.47 billion stars in Gaia early data release 3*, *AJ* **161**, 147 (2021).
- [26] M. Morii et al., *MAXI/GSC detects a possible outburst of Be/X-ray binary LS V +44 17*, *The Astronomer's Telegram* **2527**, 1 (2010).
- [27] S. Tsygankov, A. Lutovinov, R. Krivonos, *New outburst from the X-ray pulsar RX J0440.9+4431 and discovery of a possible 155 days orbital period*, *The Astronomer's Telegram* **3137**, 1 (2011).
- [28] M.H. Finger, A. Camero-Arranz, *MAXI transient confirmed to be LS V +44 17*, *The Astronomer's Telegram* **2537**, 1 (2010).
- [29] M.M. Basko, R.A. Sunyaev, *The limiting luminosity of accreting neutron stars with magnetic fields*, *MNRAS* **175**, 395 (1976).
- [30] M. Nakajima et al., *MAXI/GSC detection of an X-ray brightening from the Be/X-ray binary pulsar LS V +44 17*, *The Astronomer's Telegram* **15835**, 1 (2022).
- [31] M. Mandal et al., *NICER observation of LS V+44 17 during the record high outburst of 2022-2023*, *The Astronomer's Telegram* **15848**, 1 (2023).
- [32] S. Pal et al., *Rebrightening of 1 Crab from LS V+44 17 observed by Swift/BAT and NICER*, *The Astronomer's Telegram* **15868**, 1 (2023).
- [33] J.B. Coley et al., *Continued X-ray monitoring of LS V +44 17 with NICER, Swift/BAT, and MAXI*, *The Astronomer's Telegram* **15907**, 1 (2023).
- [34] <https://astrobrowse.issdc.gov.in/astro-archive/archive/Home.jsp>
- [35] J. Roy et al., *AstroSat science support cell*, *JA & A* **42**, 28 (2021).
- [36] H.M. Antia et al., *Large Area X-ray Proportional Counter (LAXPC) in orbit performance: Calibration, background, analysis software*, *JA & A* **42**, 32 (2021).
- [37] P.C. Agrawal, *A broad spectral band Indian Astronomy satellite 'Astrosat'*, *ASR* **38**, 2989 (2006).
- [38] K.P. Singh et al, *ASTROSAT mission*, *Proc. of SPIE* **9144**, 91441S (2014).
- [39] J.S. Yadav et al., *Large Area X-ray Proportional Counter (LAXPC) instrument onboard ASTROSAT*, *Proc. of SPIE* **9905**, 99051D (2016).
- [40] H.M. Antia et al., *Calibration of the Large Area X-Ray Proportional Counter (LAXPC) instrument on board AstroSat*, *ApJS* **231**, 1 (2017).
- [41] P.C. Agrawal et al., *Large Area X-Ray Proportional Counter (LAXPC) instrument on AstroSat and some preliminary results from its performance in the orbit*, *JA & A* **38**, 30 (2017).
- [42] J. Roy et al., *LAXPC/AstroSat study of  $\sim 1$  and  $\sim 2$  mHz quasi-periodic oscillations in the Be/X-ray binary 4U 0115+63 during its 2015 outburst*, *ApJ* **872**, 33 (2019).

- [43] J. Roy et al., *Performance of large area X-ray proportional counters in a balloon experiment*, *Exp. Astron.* **42**, 249 (2016).
- [44] <http://maxi.riken.jp/pubdata/v7.71/J0440+445/index.html>
- [45] <https://heasarc.gsfc.nasa.gov/docs/software/heasoft/>
- [46] L. Stella, L. Angelini, *XRONOS: a timing analysis software package*, Ettore Majorana international science series, Vol. 59, Data analysis in astronomy IV, ed. V.D. Gesu et al. (New York: Plenum Press), 59 (1992).
- [47] <https://heasarc.gsfc.nasa.gov/docs/software/heasoft/ftools/>
- [48] *XSPEC: The First Ten Years*, ASP conf. ser. 101, Astronomical data analysis software and systems V, ed. G.H. Jacoby & J. Barnes (San Francisco, CA: ASP), 17 (1996).
- [49] V. Jithesh et al., *Spectral and timing properties of the galactic X-ray transient Swift J1658.2-4242 using Astrosat observations*, *ApJ* **887**, 101 (2019).
- [50] A.D. Chandra et al., *Study of recent outburst in the Be/X-ray binary RX J0209.6-7427 with AstroSat: a new ultraluminous X-ray pulsar in the Magellanic Bridge?*, *MNRAS* **495**, 2664 (2020).
- [51] J. Wilms, A. Allen, R. McCray, *On the absorption of X-rays in the interstellar medium*, *ApJ* **542**, 914 (2000).
- [52] R. Misra et al., *Identification of QPO frequency of GRS 1915+105 as the relativistic dynamic frequency of a truncated accretion disk*, *ApJ* **889**, L36 (2020).
- [53] R. Rothschild et al., *Observations of the high-mass X-ray binary A 0535+26 in quiescence*, *ApJ* **770**, 19 (2013).
- [54] W. Coburn et al., *Magnetic fields of accreting X-ray pulsars with the Rossi X-ray timing explorer*, *ApJ* **580**, 394 (2002).
- [55] P.A. Becker, M.T. Wolff, *Thermal and bulk comptonization in accretion-powered X-ray pulsars*, *ApJ* **654**, 435 (2007).
- [56] R. Farinelli et al., *A new model for the X-ray continuum of the magnetized accreting pulsars*, *A&A* **591**, A29 (2016).
- [57] P. Reig, E. Nespoli, *Patterns of variability in Be/X-ray pulsars during giant outbursts*, *A&A* **551**, A1 (2013).
- [58] K. Ebisawa et al., *X-Ray spectroscopy of Centaurus X-3 with ASCA over an eclipse*, *PASJ* **48**, 425 (1996).
- [59] D.A. Liedahl, *Resonant Auger destruction and iron  $K\alpha$  spectra in compact X-ray sources*, *AIP Conf. Proc.* **774**, 99 (2005).

RX J0440.9+4431

Bin time: 10.00 s



Start Time 19955 12:23:54:581 Stop Time 19956 0:42:14:581